

On the regimes of charge reversal

Felipe Jiménez-Ángeles* and Marcelo Lozada-Cassou†
*Programa de Ingeniería Molecular, Instituto Mexicano del Petróleo,
 Lázaro Cárdenas 152, 07730 México, D. F., México*
 (Dated: May 22, 2019)

We studied charge reversal of a planar surface by a restricted primitive model electrolyte, in terms of three dimensionless independent parameters. Each of these parameters quantify one of the relevant physical effects of the system: the particles volume fraction, the ion-ion and ion-surface coulomb interactions. We study the contribution of each effect to charge reversal. As an important result we provide a simple formula to distinguish the, so-called, oscillatory and non oscillatory regimes of charge reversal. It turns out that the oscillatory regimes is independent of geometry. Our results are obtained by means of a well established integral equations theory and are in agreement with computer simulations. The agreement of our results with experiments is discussed.

PACS numbers:

I. INTRODUCTION

Charged particles naturally adsorb on an oppositely charged surface, however, temperature prevents them to completely condensate producing a diffuse layer known as the electrical double layer (EDL). Intuitively one might expect that the number of adsorbed counterions in the EDL are just the necessary to compensate the surface charge, however, for certain conditions the surface charge is *overcompensated* producing a surface *charge reversal*. When the surface *charge reversal* occurs the local electric field is inverted, thus, coions are attracted to form a second layer producing a *charge inversion* of the EDL.

Charge reversal and charge inversion have motivated a large number of studies in the last few years [1, 2, 3, 4, 5, 6]. These effects are found in the formation self-assembled polyelectrolyte layers on a charged substrate [7], electrophoresis calculations [8, 9] and experiments [10], self-assembled DNA-lipid membrane complexes [11] and anomalous macroions adsorption on a Langmuir film [12].

Charge reversal and charge inversion imply spatial oscillations of the charge distribution profiles. For bulk electrolytes, the oscillatory behavior of the ion atmosphere was predicted by Stillinger and Lovett since 1968 [13]. The oscillations of the inhomogeneous charge density profiles were observed in the early 80's [14, 15, 16, 17, 18]. In the literature two regimes for charge reversal are distinguished [19, 20]: (i) the oscillatory and (ii) non oscillatory regimes. These regimes are named according to the behavior of the electrolyte pair correlation functions in bulk. In the former regime, charge reversal is a *bulk* property and occurs for any *nonzero* surface charge density. In the second regime charge reversal is of a different nature and requires of a sufficiently high surface charge density. To the best of our knowledge the criteria

for these two regimes have not been established.

In recent computer simulations, the effect of electrostatic correlations has been studied by considering an infinitely dilute charged colloid plus an excess of counterions at *zero* temperature [21, 22, 23]. These calculations show that the system gains energy in an *overcharged* state, in which counterions adopt a Wigner crystal configuration [24, 25]. A shortcoming of these studies is, however, that the effect of short range correlations is *not* considered. For nonzero temperature and particles finite concentration, short range correlations are recognized to be important for charge reversal [3, 18, 26, 27]. Recently Messina *et al.* have shown that bidimensional ordered configurations of adsorbed particles are also induced by short range correlations [28]. In a robust mechanism for charge reversal, both, electrostatic and short range correlations should be considered.

Charge reversal is a many body effect and results from a compromise between short and long range correlations. Mechanistically, many body correlations translate in a surface-particle attractive force. Such a force is due to the particles *repulsive* electrostatic interaction and collisions, which, on a particle near the surface produce an effective force toward the surface. In Fig. 1a, the *transversal* effect of the many body repulsive forces on a single particle is represented schematically. When particles are on the surface, repulsive forces induce bidimensional order. Fig. 1b shows the effect of lateral correlations of particles on a surface.

Here we study charge reversal of a planar wall by a restricted primitive model electrolyte by means of a well established integral equations theory. Our study is based in quantifying each physical effect of the model: the particles excluded volume (entropic effect), the ion-ion and ion-wall electrostatic interactions. When the ion-wall interaction is kept constant, we found that either, the entropic contribution or the ion-ion coulomb interaction, contribute in a qualitative similar way to charge reversal. On the other hand, when the effect of the ion-wall interaction is studied we observe two opposite tendencies of charge reversal depending whether the entropic contri-

*Electronic address: fangeles@imp.mx

†Electronic address: marcelo@imp.mx

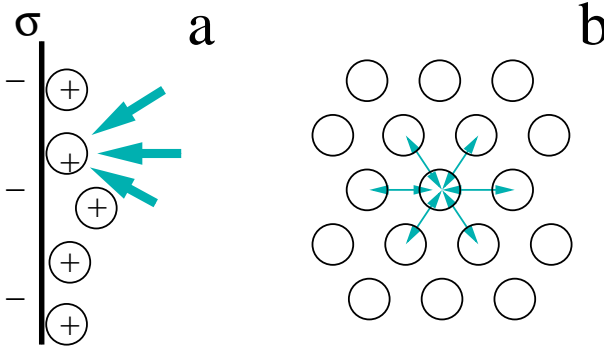


FIG. 1: (a) A diagrammatic representation of the many body *transversal* effective force on a single particle in the EDL. (b) A schematic representation of a *lateral* many body effect on an adsorbed particle. The arrows represent the repulsive electrostatic forces and collisions.

bution or the ion-ion electrostatic interaction dominate. Our study is mainly focused in studying the regimes of charge reversal, therefore, as an important result we provide a formula for a criterion that distinguish between the oscillatory and the non-oscillatory regimes of charge reversal. We also graphically study the non-oscillatory regime of charge reversal. We discuss the agreement of our study with computer simulations and experiments, as well as the discrepancies of our study with the predictions of the WC theory. The reminder of the paper is organized as follows: in section II we describe the model and theory. Section III contains the results and their discussion, and, finally, some conclusions are given in the closing part.

II. THEORY

In the Ornstein-Zernike integral equation, the correlation between two fluid particles is decomposed into direct and indirect correlations. The Ornstein-Zernike equation would involucrate the consideration of an infinite number of correlations among the particles of a thermodynamic system. However, such a consideration is not possible and the solution of the Ornstein-Zernike equation requires of *closures*. By using a closure only some of the whole number of correlations are considered. Nevertheless, in many cases, are just the necessary to properly describe some simple models for many body systems.

For inhomogeneous charged fluids, which is our concern here, the Ornstein-Zernike equation has been also applied. A particularly successful integral equations hybrid closure, that we adopt in this study, is the hypernetted chain/mean spherical approximation (HNC/MSA) [29, 30, 31].

A. The surface and fluid models

The solution of HNC/MSA is directly related with the local distribution of particles next to an external field. This approach has been applied for modelling simple and confined electrolytes in many geometries. In all these instances this approximation has proven its adequacy by showing a very good to excellent agreement with computer simulations [3, 16, 32, 33, 34]. The HNC/MSA integral equations are given by

$$g_i(\mathbf{r}_1) = \exp \left\{ -\beta u_{\alpha i}(\mathbf{r}_1) + \sum_{j=1}^2 \rho_j \int h_j(\mathbf{r}_3) c_{ij}^{MSA}(\mathbf{r}_{13}) d\mathbf{r}_3 \right\}, \quad (1)$$

Therein, $g_i(\mathbf{r}_1)$ is the ions distribution function for the species i at \mathbf{r}_1 , $h_j(\mathbf{r}_3) \equiv g_i(\mathbf{r}_3) - 1$ is the total correlation function at \mathbf{r}_3 for species j , ρ_j corresponds to the bulk number density of that ionic component and $c_{ij}^{MSA}(s)$ is the *bulk* MSA direct correlation function between two ions of the i -th and j -th types separated by $\mathbf{r}_{13} = \mathbf{r}_1 - \mathbf{r}_3$. As usual, $\beta = 1/(k_B T)$, where k_B is the Boltzmann constant and T is the absolute temperature. The ions distribution functions, are related to the ion-surface potential of mean force, $w_i(\mathbf{r}_{21})$, by $g_i(\mathbf{r}_{21}) = \exp\{-\beta w_i(\mathbf{r}_{21})\}$.

We consider an electrolyte solution contiguous to a planar wall which has a uniform surface charge density σ_0 and dielectric constant ϵ_w . In the restricted primitive model (RPM) for an electrolyte (which is the model that we adopt) the ions are taken to be hard spheres of diameter a with a centered point charge $q_i = ez_i$ (e is the protonic charge and z_i is the ionic valence), embedded in a uniform medium of dielectric constant ϵ . For simplicity we consider $\epsilon_w = \epsilon$. In planar geometry, $g_i(\mathbf{r}_1)$, depends only of the perpendicular distance to the surface, x , therefore hereinafter we will simply write $g_i(x)$. The charge on the wall is compensated by an excess of charge in the fluid given by the charge density profile, $\rho_{el}(x)$, such that

$$-\sigma_0 = \int_{a/2}^{\infty} \rho_{el}(x) dx. \quad (2)$$

The charge distribution gives the structure of the equilibrium EDL and it is expressed in terms of the ions distribution functions, $g_i(x)$, by

$$\rho_{el}(x) = \sum_{i=1}^2 z_i e \rho_i g_i(x). \quad (3)$$

The surface-ion direct interaction potential is written as $u_{\alpha i}(x) = u_{\alpha i}^{hs}(x) + u_{\alpha i}^{el}(x)$. The first term is the ion-surface hard interaction potential which considers that ions can not penetrate or deform the surface. The second

term is the electrostatic contribution which, for planar geometry, it is given by

$$u_{\alpha i}^{\text{el}}(x) = -\frac{2\pi}{\varepsilon}q_i\sigma_0(x - x_\infty), \quad (4)$$

being x_∞ the location of a reference point. The explicit form of $c_{ij}^{\text{MSA}}(s)$ for the RPM electrolyte depends only on the relative distance between two ions, $s \equiv |\mathbf{r}_{13}|$, and is written as

$$c_{ij}(s) = c^{\text{hs}}(s) + q_i q_j c^{\text{sr}}(s) - \frac{\beta q_i q_j}{\varepsilon} \frac{1}{s}, \quad (5)$$

where $c^{\text{hs}}(s)$ and $c^{\text{sr}}(s)$ are short range functions which are equal to zero for $s > a$. After a lengthy algebra, by integrating in cylindrical coordinates, Eq. (1) is written as

$$\begin{aligned} g_{\alpha i}(x) = & \exp \left\{ \frac{4\pi\beta}{\varepsilon} z_i e \sigma_0 x + 2\pi \int_{a/2}^{\infty} K(x, y) h_{\alpha s}(y) dy \right. \\ & + J(x) + 2\pi z_i \int_{a/2}^{\infty} L(x, y) h_{\alpha d}(y) dy \\ & \left. + \frac{2\pi\beta e^2 z_i}{\varepsilon} \int_{a/2}^{\infty} h_{\alpha d}(y) [x + y + |x - y|] dy \right\}, \end{aligned} \quad (6)$$

with $i = 1, 2$ and defining $h_{\alpha s}(y) \equiv \sum_{m=1}^2 \rho_m h_{\alpha m}(y)$, $h_{\alpha d}(y) \equiv \sum_{m=1}^2 z_m \rho_m h_{\alpha m}(y)$ and

$$\begin{aligned} K(x, y) & \equiv \int_{|x-y|}^{\infty} c_s(s) s ds \\ L(x, y) & \equiv \int_{|x-y|}^{\infty} c_d^{\text{sr}}(s) s ds. \\ J(x) & \equiv -2\pi\rho_T \int_{x-a}^{a/2} K(x, y) dy. \end{aligned}$$

where $\rho_T = \sum_{i=1}^2 \rho_i$ and it has been used that $h_{\alpha i} = -1$ for $x \leq a/2$. The HNC/MSA Eq. (6) integral equations can be conveniently written as

$$g_i(x) = \exp\{-\beta w_i(x)\} = \exp\{-\beta q_i \psi(x) + w_i^{\text{sr}}(x)\}. \quad (7)$$

From here, it is seen that $w_i(x)$ has two contributions: the mean electrostatic potential, $\psi(x)$, expressed as

$$\psi(x) = -\frac{4\pi}{\varepsilon}\sigma_0 x - \frac{2\pi}{\varepsilon} \int_{a/2}^{\infty} \rho_{\text{el}}(y) [x + y + |x - y|] dy, \quad (8)$$

and a short range *excluded volume* potential

$$\begin{aligned} w_i^{\text{sr}}(x) = & 2\pi \int_{a/2}^{\infty} K(x, y) h_{\alpha s}(y) dy + J(x) \\ & + 2\pi z_i \int_{a/2}^{\infty} L(x, y) h_{\alpha d}(y) dy \end{aligned} \quad (9)$$

In the case of $q_i = 0$, the fluid is a hard spheres fluid. Thus, $\psi(x) = 0$ and only the short range terms are included in Eq. (7). On the other hand, in the point ions limit Eq. (7) becomes

$$\begin{aligned} g_i(x) = & \exp\{-\beta q_i \psi(x)\} = \exp \left\{ \frac{2\pi}{\varepsilon} \sigma_0 \beta q_i x \right. \\ & \left. + \frac{4\pi}{\varepsilon} \beta q_i \int_{a/2}^{\infty} \rho_{\text{el}}(y) [x + y + |x - y|] dy \right\}, \end{aligned} \quad (10)$$

which is the integral version of the PB equation. For $a = 0$ $w_i^{\text{sr}}(x) = 0$, i. e., in PB theory the short range correlations are not included.

B. The relevant parameters

Several physical contributions rule charge reversal. One of them is the surface-particle direct interaction, which at the surface it is given by $U_i = q_i u_{\gamma i}(\frac{a}{2}) = \frac{2\pi q_i \sigma}{\varepsilon} (x_\infty - \frac{a}{2})$. The more negative the value of U_i , particles adsorption is energetically more favorable. Several important effects are beyond this simple contribution. Many body correlations induce a surface-particle attractive forces of a different nature. The physical contributions to many body correlations are the particles accessible volume and the *strength* of the ion-ion electrostatic interaction. From Eq.(6) we define the following parameters:

$$\eta \equiv \frac{\pi}{6} \rho_T a^3, \quad \xi \equiv \frac{q^2 \beta}{a \varepsilon}, \quad \text{and} \quad \gamma_i \equiv \frac{2\pi \beta}{\varepsilon} q_i \sigma_0 a,$$

where $q_i = z_i e$ and $q = |z_i| e$. The parameters ξ and Γ quantify the ion-ion and ion-surface interaction, respectively, and η is the particles volume fraction. Thus, Eq.(4) is written as

$$-\beta u_{\alpha i}(X) \equiv \frac{1}{2} \gamma_i (X - X_\infty), \quad (11)$$

with $X \equiv 2x/a$ the dimensionless distance, Eq. (6) is written as

$$\begin{aligned} g_i(X) = & \exp \left\{ \gamma_i X + \int_1^{\infty} \hat{h}_{\alpha s}(Y) \hat{K}(X, Y) dY \right. \\ & + \hat{J}(X) + \hat{z}_i \xi \int_1^{\infty} \hat{h}_{\alpha d}(Y) \hat{L}(X, Y) dY \\ & \left. + 3\hat{z}_i \xi \int_1^{\infty} \hat{h}_{\alpha d}(Y) [X + Y + |X - Y|] dY \right\}, \end{aligned} \quad (12)$$

where $\hat{z}_j \equiv q_j/q$ and we have defined

$$\begin{aligned} \hat{h}_{\alpha s}(X) & = \sum_{m=1}^n \eta_m h_{\alpha m}(X), \\ \hat{h}_{\alpha d}(X) & = \sum_{m=1}^n \hat{z}_m \eta_m h_{\alpha m}(X). \end{aligned}$$

The expressions for $\hat{K}(X, Y)$, $\hat{L}(X, Y)$ and $\hat{J}(X)$ are given below. For $X - 2 \leq Y \leq X + 2$,

$$\begin{aligned}\hat{K}(X, Y) &= \frac{3}{4}c_1[(X - Y)^2 - 4] + \frac{3}{2}\eta c_2[|X - Y|^3 - 8] \\ &+ \frac{3}{160}\eta c_1[|X - Y|^5 - 32] \\ \hat{L}(X, Y) &= 3[2 - |X - Y|] - \frac{3}{2}\frac{\Gamma a}{(1 + \Gamma a)}[4 - (X - Y)^2] \\ &+ \frac{1}{4}\left(\frac{\Gamma a}{1 + \Gamma a}\right)^2[8 - |X - Y|^3]\end{aligned}$$

otherwise $\hat{K}(X, Y) = \hat{L}(X, Y) = 0$. For $1 \leq X \leq 3$

$$\begin{aligned}\hat{J}(X) &= \frac{1}{4}\eta c_1[\hat{p}^3 - 12\hat{p} + 16] + \frac{3}{8}\eta^2 c_2[\hat{p}^4 - 32\hat{p} + 48] \\ &+ \frac{1}{320}\eta^2 c_1[\hat{p}^6 - 192\hat{p} + 320],\end{aligned}$$

otherwise $\hat{J}(X) = 0$, with $\hat{p} \equiv X - 1$. We solve HNC/MSA [Eq. (12)] using a sophisticated finite element technic, as a result, we obtain the ions reduced concentration profiles $g_i(X)$.

III. RESULTS AND DISCUSSION

For the study of the mechanisms leading to charge reversal, the local electric field is useful to identify and quantify charge reversal. By Gauss law, the electric field is given by

$$E(x) = \frac{2\pi}{\varepsilon}[\sigma_0 + \sigma'(x)], \quad (13)$$

being $\sigma'(x)$ the accumulated charge between a plane parallel to the surface at $a/2$ and a parallel plane at a distance x from the plate, given by

$$\sigma'(x) = \int_{a/2}^x \rho_{el}(x)dx. \quad (14)$$

The electroneutrality condition implies that $\lim_{x \rightarrow \infty} \sigma'(x) = -\sigma_0$, such that the electric field produced by the plate is completely screened at infinity. In order to evaluate charge reversal we conveniently define the dimensionless function

$$\sigma(x) \equiv -\frac{\sigma_0 + \sigma'(x)}{\sigma_0}, \quad (15)$$

such that charge reversal occurs in an interval $[x_1, x_2]$ where $\sigma'(x)$ overcompensates σ_0 , or equivalently $\sigma(x) > 0$. We define

$$\sigma^* \equiv \max\{\sigma(x) : x \in [a/2, \infty)\} \quad (16)$$

or, in other terms

$$\sigma^* = -1 - \frac{1}{\sigma_0} \int_{a/2}^{x_{max}} \rho_{el}(x)dx \quad (17)$$

where $x_{max} \in [a/2, \infty)$ is the the location of the absolute maximum of $\sigma(x)$. σ^* measures the *excess* of adsorbed charge per unit of surface charge and, by definition, $\sigma^* \geq 0$. Our definition of σ^* is equivalent to that for σ_{WC}^* given in Eq. (1) in ref. [25]. It turns out that in the symmetric RPM electrolyte x_{max} is defined by $\rho_{el}(x_{max}) = 0$.

Our first task is to delimitate the precise conditions for which charge reversal occurs. From a primary exploration in terms of η , ξ and γ , we found the following: (i) for moderately low values of the γ parameter (typically $\gamma < 1$) a successive increasing of *any* of both parameters (η or ξ) eventually produces charge reversal. (ii) When η and ξ are *low* a successive increasing of γ eventually produces charge reversal. The former result suggested to scan all the possible combinations of η and ξ for which charge reversal occurs keeping constant the value of $\gamma < 1$. We carried out the scanning by successive increasing of both ξ and η . In Fig. 2 it is sketched a diagram in the ξ - η plane of the set of points where it is satisfied that $\sigma^* > 0$. The continuous line represents a boundary limit above which charge reversal occurs and always increases by increasing η and ξ . This boundary line is numerically defined by the condition $\sigma^* \geq 10^{-6}$ which, however, might be undetectable by computer simulations or by experiments. The conditions for a higher charge reversal will be discussed below. An interesting finding was that for successive similar calculations for lower values of γ produced exactly the *same* curve. Carrying out a similar procedure in cylindrical and spherical geometries we found that this boundary line is the also the same. Therefore, we partially concluded that for low values of the surface charge density (or equivalently $\gamma < 1$) the boundary line is independent of the surface charge density and geometry. The parameter γ , however, is functionally different in the spherical and planar geometries.

We fitted a function to the curve of Fig. 2 and we found that it satisfies $\eta\xi = 0.066$, or equivalently $24\xi\eta = \kappa^2 a^2 = 1.6$, with $\kappa^2 = \frac{4\pi}{\epsilon} \sum_{i=1}^2 q_i^2 \rho_i$. Thus, this curve splits the ξ - η plane into regimes: In regime I (for $\xi\eta > 0.066$), charge reversal occurs for any non-zero value of σ_0 . *This condition defines the so called oscillatory regime*. In regime II (for $\xi\eta < 0.066$), the occurrence of charge reversal strongly depends on the γ parameter and corresponds to the non-oscillatory regime. Although some authors [19, 35] endorsed the existence of such regimes, they did not provided the criteria to distinguish these regimes. In regime I there is not a minimum value of σ_0 (or γ) to produce charge reversal. This fact is in opposition to the Wigner crystal theory prediction [36] in which a relatively high value of σ_0 and z is needed to produce charge reversal. The localization of some typical electrolyte solutions is also displayed in this diagram. Notice that the 2:2, 0.5M and the 1:1, 1M and 2M electrolytes are clearly on regime I.

As we pointed out above, in regime II ($\xi\eta < 0.066$), a minimal surface charge density is required to produce charge reversal. In a similar way as for Fig. 2, we carried

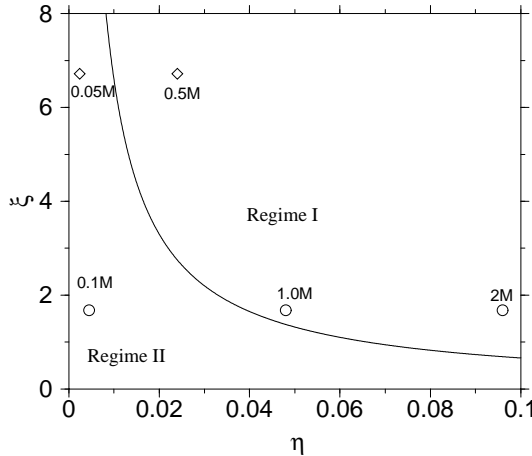


FIG. 2: Diagram in the ξ - η plane. The curve delimits regimes I and II of charge reversal. The white diamonds are for a 2:2, 0.05M (left) and 0.5M (right) electrolytes. The white circles are for a 1:1, 0.1M (left), 1M (center) and 2.0M (right) electrolytes. Both, circles and diamonds, are for $a = 4.25\text{\AA}$, $T = 298\text{K}$, $\epsilon = 78.5$

out an scanning by successive increasing of the value of $\xi\eta$ and γ . In Fig. 3 it is sketched a typical diagram in the γ - $\xi\eta$ plane of the set of points where first it is satisfied that $\sigma^* > 0$. This curve defines the sub-regimes IIa and IIb. Above the line (sub-regime IIa) charge reversal occurs whereas below (sub-regime IIb) charge reversal does not occurs. In this regime such a boundary line will depend on the specific electrolyte defined by the parameters ξ . However, all the curves satisfy that $\lim_{\xi\eta \rightarrow 0} \gamma \rightarrow \infty$ and $\lim_{\xi\eta \rightarrow 0.066} \gamma \rightarrow 0$. In particular the example shown in Fig. 3 corresponds to a divalent electrolyte in aqueous solution (with $a = 4.25\text{\AA}$, $\epsilon = 78.5$, $T = 298\text{K}$) $\xi = 6.72$ and a successive increasing of the product $\xi\eta$ implies an increasing of the electrolyte concentration. Notice (in the right hand side scale) the *high* values of the required equivalent surface charge density. Figs. 2 and 3 show that the occurrence of charge reversal requires of a compromise between short and long range correlations. These two diagrams are helpful in studying the regimes of charge reversal and to locate the precise conditions for the occurrence of charge reversal.

Recently Shklovskii *et al.* have considered charge reversal of charged surface by *oppositely* charged macroions [25]. They proposed that the *highly* charged macroions overscreening a *highly* charged surface, are ordered in a bidimensional Wigner crystal (WC) structure. However, in their theory ionic correlations are only considered as for a two dimensional screened electrons liquid at *zero* temperature. In WC theory, Shklovskii *et al.* found that charge reversal (quantified by σ_{WC}^* which has a similar meaning to σ^* given in Eq. (16)) increases monotonically with $\zeta_{WC} = ze/\sigma_0\pi r_s^2$, having z and σ_0 the same meaning as in this work and being r_s the Debye screening length. Although charge reversal is partially governed by

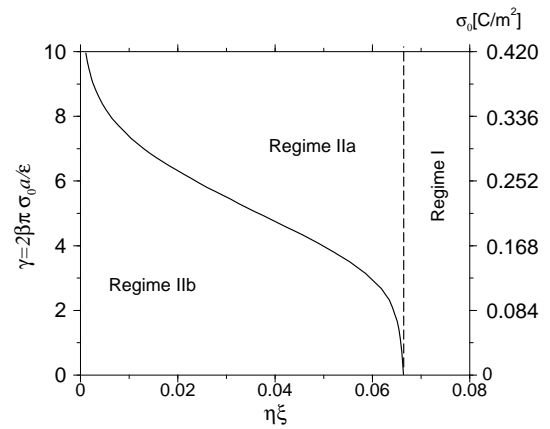


FIG. 3: Diagram in the γ - $\xi\eta$ plane in which the boundary continuous line defines regimes IIa and IIb. Charge reversal occurs in regime IIa. The continuous boundary line was computed for a fixed value of $\xi = 6.72$ which correspond to a divalent electrolyte with $a = 4.25\text{\AA}$, $T = 298\text{K}$, $\epsilon = 78.5$. The dashed line splits the space in regimes I and II and is at $\xi\eta = 0.066$. In the right hand side it is shown the scale for σ_0 .

the repulsive electrostatic interactions, the no inclusion of hard core correlations in WC theory makes it inappropriate describe charge reversal. Fig. 4 has been produced for a fixed values of $\xi = 6.72$ and $\gamma = 2.4$ and shows different curves of $P(x)$ for successive increasing values of η . This plot shows that charge reversal increases as η increases. This behavior is not supported by the WC theory.

In the inset of Fig. 4, σ^* is plotted as a function of

$$\zeta \equiv \frac{\xi\eta}{\gamma} = \frac{zen}{2\pi\sigma_0a^2}. \quad (18)$$

Please note the similarity between ζ with the parameter $\zeta_{WC} = ze/\sigma_0\pi r_s^2$ used in the WC theory [24, 25]. This curve was produced from the maxima of the σ 's functions in the main plot in which ξ and γ are kept constant ($ze/2\pi\sigma_0a^2 = 2.8$) and η has been increased successively. We observe that σ^* increases monotonically by increasing η and keeping constant ξ and γ (continuous line at the inset). A qualitatively similar behavior is obtained if ξ is increased and η is kept constant (dashed line at the inset). Our results show that *charge reversal* is increased by increasing either the coulombic coupling (ξ) or the particles volume fraction (η). This plot seems to be qualitatively similar with the prediction of WC theory (Fig. 3 in Ref. [25]), however, in WC theory σ^* does not depend on η and, thus, does *not* predict the increasing of σ^* by increasing η .

In the WC theory it is predicted that σ^* always increases monotonically by increasing ζ_{WC} . This implies that charge reversal will increase by increasing z or by decreasing σ_0 . We have shown that σ^* increases monotonically by increasing $\zeta = \xi\eta/\gamma$ keeping γ constant, which

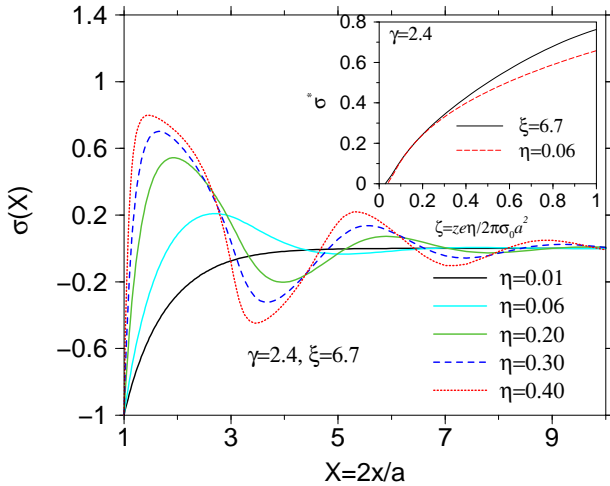


FIG. 4: $P(X)$ for successively increasing values of η and constant values of $\xi = 6.7$, and $\gamma = 2.4$. In the inset it is shown a plot of σ^* as a function of $\zeta = \xi\eta/\gamma = z\eta/2\pi\sigma_0a^2$, for $\gamma = 2.4$. The continuous line correspond to $\xi = 6.72$ and increasing values of η , whereas the dashed line is for $\eta = 0.06$ and increasing values of ξ .

is equivalent to increase z or η . We now analyze the effect of γ (or equivalently σ_0) on σ^* . In Fig. 5 we have plotted σ^* vs ζ . Each curves has been produced keeping constant ξ and η (z , ρ and a), imposing the following constrain $\xi\eta = 0.220$. In this plot we distinguish two tendencies in the plot of σ^* vs ζ : the first which we denote as coulombic and the second as entropic. The former is characterized by a dominant coulombic contribution (ξ). The dot-dashed and dotted line follow the coulombic trend, in which σ^* decreases by increasing ζ (decreasing σ_0). The entropic behavior is characterized by a dominant contribution of the particles volume fraction (η). The continuous and dashed lines follow an entropic trend, in which σ^* increases by increasing ζ (decreasing σ_0). Although WC theory predicts qualitatively a similar tendency in the plot of σ_{WC}^* vs ζ_{WC} , in our study this behavior requires of an important contribution of the hard-core many body correlation, which is precisely what WC theory neglects.

Both trends, coulombic and entropic, are supported by computer simulations in studies of charge reversal in cylindrical [3] and spherical geometries [28], however, more important is the qualitative agreement with experimental results. In an experiment of ion adsorption on a Langmuir film made of amphiphilic molecules, the surface charge density can be increased by decreasing the surface area per amphiphilic molecule. In this kind of experiments, Rondelez [12] found that ions adsorption increases (hence charge reversal increases) as the lipid layer

charge density decreases. This is consistent with the plot of σ^* vs ζ in Fig. 5 (for the entropic tendency) where a decrement of the surface charge density decreases charge reversal but not the ions adsorption which is strongly driven by particles excluded volume.

IV. CONCLUSIONS

We studied charge reversal (*charge reversal*) of a planar surface by a restricted primitive model electrolyte. The physical contributions of the system are quantified by a set of three independent dimensionless parameters, given by $\eta = \frac{\pi}{6}\rho_T a^3$, $\xi = \frac{\beta q^2}{\epsilon a}$ and $\gamma = 2\pi q\beta\sigma_0a/\epsilon$. The former quantifies the particles volume fraction and the second and third parameters account for the ion-ion and ion-surface coulomb interactions, respectively. Within this parametric description, we confronted the effects of excluded volume vs coulomb coupling in an study of (*charge reversal*). From this study results a general criterion between the oscillatory and non-oscillatory regimes of charge reversal: the oscillatory regime is defined by the condition $\xi\eta = \frac{1}{24}\kappa^2a^2 > 0.066$, being κ the inverse Debye length. In this regime, *charge reversal* occurs for any non-zero surface charge density. In the non oscillatory regime (defined by $\xi\eta < 0.066$), charge reversal strongly depends on the surface charge density σ_0 (given by the value of γ). In this regime we presented a diagram for a typical electrolyte which distinguishes the conditions for charge reversal. There is not, however, a single general criterion for charge reversal in regime II.

Our study of the mechanisms of charge reversal for a *non-zero* temperature system shows that charge reversal results from a compromise between short range and electrostatic correlations. We showed that σ^* (which quantifies charge reversal) increases in a qualitatively similar way by increasing either η or ξ . This in turn indicates that short range correlations contribute to charge reversal in a similar way as electrostatic correlations. In our analysis of the effect of the external field, which is quantified by γ parameter, we found two tendencies in the plots of σ^* vs $\zeta = \xi\eta/\gamma$, in which the value of $\xi\eta$ is kept constant. In the entropic trend (η dominant) we found that σ^* increases by increasing ζ (decreasing γ or equivalently σ_0). On the other hand when ξ is dominant (coulombic tendency) we found that σ^* decreases by increasing ζ . These tendencies are supported by computer simulations studies of charge reversal in cylindrical [3] and spherical geometries [28], but more importantly, in qualitative agreement with experimental results [12]. The predictions of our study, however, do *not* match with the predictions of the WC theory in which σ_{WC}^* is described in terms of a single parameter ζ_{WC} .

[1] W. M. Gelbart, R. F. Bruinsma, P. A. Pincus, and V. A. Parsegian, Physics Today **53**, 38 (2000).

[2] P. Attard, J. Phys. Chem. **99**, 14174 (1995).

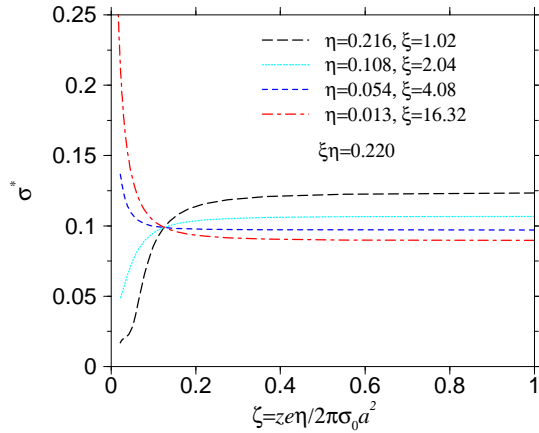


FIG. 5: σ^* as a function of $\zeta = \xi\eta/\gamma = z\eta/2\pi\sigma_0a^2$, in which each curve is calculated with different combinations of ξ and η but in all cases it is satisfied $\xi\eta = 0.220$. In these curves an increasing of ζ implies a decreasing of γ or equivalently a decreasing of σ_0 .

- [3] M. Deserno, F. Jiménez-Ángeles, C. Holm, and M. Lozada-Cassou, *J. Phys. Chem. B* **105**, 10983 (2001).
- [4] M. Tanaka and A. Y. Grosberg, *J. Chem. Phys.* **115**, 567 (2001).
- [5] T. Terao and T. Nakayama, *Phys. Rev. E* **63**, 041401 (2001).
- [6] T. Terao and T. Nakayama, *Phys. Rev. E* **65**, 021405 (2002).
- [7] G. Decher, *Science* **277**, 1232 (1997).
- [8] M. Lozada-Cassou, E. González-Tovar, and W. Olivares, *Phys. Rev. E* **60**, R17 (1999).
- [9] M. Lozada-Cassou and E. González-Tovar, *J. Coll. Int. Sci.* **239**, 285 (2001).
- [10] M. Quesada-Pérez *et al.*, *Chem. Phys. Chem.* **4**, 234 (2002).
- [11] J. O. Rädler, I. Koltover, T. Salditt, and C. R. Safinya, *Science* **275**, 810 (1997).
- [12] N. Cuvillier and F. Rondelez, *Thin Solid Films* **327-329**, 19 (1998).
- [13] F. H. Stillinger and R. Lovett, *J. Chem. Phys.* **48**, 3858 (1968).

- [14] W. van Megen and I. Snook, *J. Chem. Phys.* **73**, 4656 (1980).
- [15] L. B. Bhuiyan, C. W. Outhwaite, and S. Levine, *Mol. Phys.* **42**, 1271 (1981).
- [16] M. Lozada-Cassou, R. Saavedra-Barrera, and D. Henderson, *J. Chem. Phys.* **77**, 5150 (1982).
- [17] G. M. Torrie and J. P. Valleau, *J. Phys. Chem.* **86**, 3251 (1982).
- [18] E. Gonzales-Tovar, M. Lozada-Cassou, and D. Henderson, *J. Chem. Phys.* **83**, 361 (1985).
- [19] P. Attard, *J. Phys. Chem.* **99**, 14174 (1995).
- [20] H. Greberg and R. Kjellander, *J. Chem. Phys.* **7**, 2940 (1998).
- [21] R. Messina, C. Holm, and K. Kremer, *Phys. Rev. Lett.* **85**, 872 (2000).
- [22] R. Messina, C. Holm, and K. Kremer, *Europhys. Lett.* **51**, 461 (2000).
- [23] R. Messina and C. Holm and K. Kremer, *Phys. Rev. E* (in press).
- [24] T. T. Nguyen, A. Y. Grosberg, and B. I. Shklovskii, *J. Chem. Phys.* **113**, 1110 (2000).
- [25] T. T. Nguyen, A. Y. Grosberg, and B. I. Shklovskii, *Phys. Rev. Lett.* **85**, 1568 (2000).
- [26] M. Lozada-Cassou and F. Jiménez-Ángeles, *arXiv:physics* **v2**, 0105043 (2001).
- [27] F. Jiménez-Ángeles and M. Lozada-Cassou, *arxiv* **1**, condmatt0303519 (2003), submitted.
- [28] R. Messina, E. González-Tovar, M. Lozada-Cassou, and C. Holm, *Europhys. Lett.* **60**, 383 (2002).
- [29] M. Lozada-Cassou, in *Fundamentals of inhomogeneous fluids*, edited by D. Henderson (Marcel Dekker, New York, 1993), Chap. 8.
- [30] M. Lozada-Cassou, *J. Chem. Phys.* **75**, 1412 (1981).
- [31] M. Lozada-Cassou, *J. Chem. Phys.* **80**, 3344 (1984).
- [32] L. Degrève, M. Lozada-Cassou, E. Sánchez, and E. González-Tovar, *J. Chem. Phys.* **98**, 8905 (1993).
- [33] J. Yu and M. Lozada-Cassou, *Phys. Rev. Lett.* **79**, 3656 (1997).
- [34] L. Degrève and M. Lozada-Cassou, *Phys. Rev. E* **57**, 2978 (1998).
- [35] H. Greberg and R. Kjellander, *J. Chem. Phys.* **108**, 2940 (1998).
- [36] B. I. Shklovskii, *Phys. Rev. E* **64**, 041407 (1999).